On the causes and dynamics of the early twentieth century North American pluvial

Benjamin I Cook *

NASA Goddard Institute for Space Studies, NY, NY, USA

Richard Seager

Lamont-Doherty Earth Observatory, Palisades, NY, USA

Ron L Miller

NASA Goddard Institute for Space Studies, NY, NY, USA

---

* *Corresponding author address:* Benjamin I Cook, NASA Goddard Institute for Space Studies, 2880 Broadway, New York, NY 10025.

E-mail: bc9z@ldeo.columbia.edu

ABSTRACT

The early twentieth century North American pluvial (1905-1917) was one of the most extreme wet periods of the last five hundred years and directly led to overly generous water allotments in the water-limited American West. Here we examine the causes and dynamics of the pluvial event using a combination of observation-based data sets and general circulation model (GCM) experiments. The character of the moisture surpluses during the pluvial differed by region, alternately driven by increased precipitation (the southwest), low evaporation from cool temperatures (the central plains), or a combination of the two (the Pacific northwest). Cool temperature anomalies covered much of the west and persisted through most months, part of a globally extensive period of cooler land and sea surface temperatures (SST). Circulation during boreal winter favored increased moisture import and precipitation in the southwest, while other regions and seasons were characterized by near normal or reduced precipitation. Anomalies in the mean circulation, precipitation, and SST fields are only partially consistent with the relatively weak El Niño forcing during the pluvial, suggesting a significant role for internal variability or other forcing agents. Differences between the reanalysis dataset, an independent statistical drought model, and GCM simulations highlight some of the remaining uncertainties in understanding the full extent of SST forcing of North American hydroclimatic variability.

1. Introduction

The development of western North America (NA) during the twentieth century was largely made possible through human appropriation of natural water flows for industrial, municipal, and agricultural uses (e.g., Barnett and Pierce 2009; Christensen et al. 2004; Sophocleous 2010; Reisner 1993; Worster 1992). One set of appropriations is legally formalized under the Colorado River Compact (CRC) of 1922 (Christensen et al. 2004; MacDonnell et al. 1995), an international agreement that apportioned discharge from the Colorado River between the states in the Upper (Wyoming, Utah, Colorado, New Mexico) and Lower (California, Arizona, Nevada) Colorado River basins and Mexico (Christensen et al. 2004). The CRC apportionments are based on estimated climatological discharge at Lee's Ferry on the Colorado River of 22 billion cubic meters (BCM), using baseline flows from the early twentieth century (Christensen et al. 2004). As development in the west continued, and as the long term hydroclimate in the west was clarified with longer instrumental records and paleoclimate reconstructions (Fye et al. 2003; Meko et al. 2007; Stockton and Jacoby 1976; Woodhouse et al. 2005), the overly generous nature of the original CRC allocations became apparent. For example, mean annual discharge at Lee's Ferry calculated over a much longer interval (1906-2000) was only 18.6 BCM, ranging in any given year from 6.5 BCM to 29.6 BCM (Christensen et al. 2004). The reconstructed climatology extending back to 1512 C.E. is even lower (16.7 BCM), making it highly likely that the flows that formed the basis for the CRC were higher than the climatological baseline for the last 500 years (Christensen et al. 2004; Fye et al. 2003).

The exceptionally high flow during the early twentieth century coincided with anomalous wet conditions throughout the west, spanning approximately 1905-1917, a period generally referred to as the early twentieth century pluvial (the term pluvial referring to wetter than normal conditions) (e.g., Fye et al. 2003, 2004; Woodhouse et al. 2005). This was the most persistent pluvial event in the west to occur during the twentieth century, and recent drought reconstructions based on networks of tree ring chronologies suggest it may have been the wettest period in the west anytime in the last thousand years (Cook et al. 2004). An analysis of temperature and precipitation records from the time suggested that the pluvial (as reflected in river discharge and drought metrics) arose from a combination of anomalously high winter-time precipitation and reduced evaporation from cooler than normal warm season temperatures (Woodhouse et al. 2005).

To date, few studies have discussed the underlying dynamics or causes of the early twentieth century pluvial. Fye et al. (2004) suggested that anomalously cool temperatures in the North Pacific and warm conditions in the tropical Pacific would have favored increased moisture flux into the southwest, although this was speculative because of the absence at the time of atmospheric circulation datasets covering this time period. Since then, however, new datasets and model simulations have become available, leaving us poised for an in-depth investigation into the causes of the early twentieth century pluvial in western NA. Here, we use available datasets and an ensemble of general circulation model (GCM) simulations to investigate the North American pluvial (1905-1917) and assess 1) the relative importance of temperature versus precipitation for the pluvial moisture surpluses, 2) the dynamics underlying these anomalies, and 3) the importance of sea surface temperature (SST) forcing during this interval.

2. Methods and Data

Our analysis will use observation-based data sets and a suite of GCM experiments to investigate the physics and dynamics underlying the spatial structure and temporal evolution of the pluvial event. We divide the west into three regions separated by their own distinct climatologies and SST-drought teleconnections. Despite these differences, all three regions experienced significant wet conditions during the pluvial. The regions are the southwest (SW, 125°W-103°W, 25°N-42°N), the northwest (NW, 125°W-103°W, 42°N-50°N), and the central plains (CP, 103°W-90°W, 35°N-50°N). These regions are outlined in Figure 1 and other subsequent figures.

a. Palmer Drought Severity Index

Droughts and pluvials may be defined in a variety of ways, depending on the research question of interest (Dracup et al. 1980). At the core of all definitions, however, is the concept of a moisture deficit (droughts) or surplus (pluvials). While these surpluses and deficits are typically viewed primarily as a consequence of moisture supply (i.e., precipitation), they may also strongly depend upon evaporative demand. One drought index that incorporates information on moisture supply (via precipitation) and evaporative demand (as a function of temperature) is the Palmer Drought Severity Index (PDSI) (Palmer 1965). PDSI is a normalized drought index typically ranging from -5 to +5, with positive values indicating wetter than normal conditions (pluvials) and negative values indicating drier conditions (droughts). Because PDSI is locally normalized around a mean of zero, the PDSI anomalies between different regions are directly comparable.

We use two different PDSI datasets in our analysis. The first is the North American Drought Atlas (NADA) version 2a (http://www.ncdc.noaa.gov/paleo/pdsi.html) (Cook et al. 2007), a tree-ring proxy-based reconstruction of PDSI covering much of North America. The NADA product reconstructs PDSI for the summer (June-July-August) season using 1,821 tree ring chronologies, over as many as 286 2.5°x2.5° grid-boxes. This product is well-validated and versions of the NADA have been used in other studies of NA drought variability (Cook et al. 1999, 2004, 2007; Fye et al. 2003; Herweijer et al. 2007). We use the NADA to examine the spatial extent and intensity of the pluvial and also place the pluvial anomalies within the context of moisture variability over the last five hundred years. We also calculate a second set of PDSI values directly from available gridded monthly temperature and precipitation data (see below). We use this second dataset to look at the relative contribution of the PDSI anomalies during the pluvial by temperature versus precipitation.

b. Temperature and Precipitation

Gridded temperature and precipitation data are taken from version 2.1 of the Climate Research Unit (CRU) monthly climate grids (Mitchell and Jones 2005). The CRU data are statistically interpolated from monthly station observations to a regular terrestrial grid at half degree spatial resolution and monthly temporal resolution, covering the time period 1901-2002. We use these data to look at seasonal temperature and precipitation anomalies during the pluvial and also use them in our own calculation of PDSI. We also use SST data from the Hadley Centre (HadISST; Rayner et al. 2003) and a dataset of global and hemispherically averaged temperature for the last 150 years (HadCRUTv3; Brohan et al.

2006). A measure of the El Niño Southern Oscillation (ENSO), the NINO3.4 index, is also calculated from the HadISST dataset. Unless otherwise indicated, all temperature and precipitation anomalies are expressed relative to a 1961-1990 climatology. We recognize that there may be issues using this baseline period because of the strong warming trends over the twentieth century. However, we note that 1) this time period is still often used as the standard baseline in climate analyses, 2) data during this period is relatively well sampled spatially and temporally, and 3) it is difficult to develop a comprehensive baseline prior to the pluvial period and major warming trends.

c. Atmospheric Circulation

Data on atmospheric circulation and dynamics are taken from the Twentieth Century Reanalysis Project (Compo et al. 2006, submitted; Whitaker et al. 2004). This product covers the time span 1871-2008, using a data assimilation model forced by observed climate forcings and SSTs (from HadISST). This reanalysis only assimilates surface and sea level pressure observations, but has been used to investigate early twentieth century circulation features (e.g., Cook et al. 2010; Wood and Overland 2009).

d. GCM Experiments

We also use results from a 16-member ensemble of atmosphere GCM simulations forced with observed SSTs to determine the extent to which SST forcing may be able to explain climate anomalies during the pluvial. These simulations cover 1856 to the near present, and have been previously used to investigate SST forcing of drought over NA with good success

(Seager et al. 2005b; Seager 2007). The SST forcing comes from Kaplan et al. (1998) for the tropical Pacific Ocean for the entire period and, where available, for 1856-1870, and from the Hadley center (Rayner et al. 2003) outside of the tropical Pacific from 1871 on. The GCM is the Community Climate Model version 3 (CCM3), developed at the National Center for Atmospheric Research (Kiehl et al. 1998). The model runs are referred to as GOGA for Global Ocean Global Atmosphere.

3. Results

a. The Pluvial in a Long-term context

Anomalous wet conditions were widespread throughout western NA during the pluvial, with positive PDSI anomalies spanning from Mexico to southern Canada and from the Pacific coast across the Great Plains (Figure 1). The largest PDSI anomalies (+3 and greater) are concentrated along an axis extending from the southwest into the northwest and northern plains. Notably, there are no drought conditions (PDSI <-1) anywhere during this time period, at least in the multi-year average.

All three regions are characterized by high moisture variability and persistent drought and pluvial periods (Figure 2); time series are smoothed (5 year lowess filter) to emphasize persistent events. Twentieth-century drought events are well-resolved by the PDSI anomalies, including the well-documented droughts in the 1950s (SW) and the 1930s ‘Dust Bowl’ (NW and CP), as well as the multi-decadal ‘megadroughts’ in previous centuries. Compared to other pluvial intervals over the last five hundred years, the early twentieth century event generally stands out through a combination of its intensity, duration, and spatial extent. In all three regions, the time evolution of the pluvial indicates two wet phases, with a break towards dry or near normal conditions around 1910. The break in 1910 corresponds to La Niña conditions in the tropical Pacific, a situation that typically suppresses precipitation in southwestern NA and the southern Great Plains. Over the CP region, the pluvial appears to have started earlier than in either the SW or NW, and the post 1910 phase of the pluvial also appears weaker in this region.

b. Temperature and Precipitation During the Pluvial

Temperature anomalies were generally cool throughout the west, especially during the spring (MAM) and summer (JJA) peak evaporative seasons (Figure 3). The west was also cooler than normal during winter (DJF), with the exception of slightly warmer than normal conditions over California. The largest positive precipitation anomalies occurred in the SW during winter, with increases on the order of 50-60% (Figure 4). During DJF there were also wet anomalies in the CP, but these were relatively low in absolute terms because the annual cycle in precipitation over this region peaks in the summer. What may be even more remarkable is how many regions experienced precipitation deficits during the pluvial, especially the SW during JJA and SON, the NW during DJF, and the CP during MAM. This supports the hypothesis (Woodhouse et al. 2005) that cool temperature anomalies and low evaporative demand may be as important as precipitation for explaining the large moisture surpluses reflected in the positive PDSI values.

A look at the actual temperature (K) and precipitation (mm day^{-1}) anomalies averaged over the three western regions during the pluvial provides some further insight (Figure 5). Overlain in the precipitation plots is a scaled down (60%) version of the NINO3.4 index (dashed line). When NINO3.4 is strongly positive, this is indicative of warm-phase El Niño events generally associated with increased winter and spring precipitation in the southwest and decreased precipitation during the same seasons in the northwest. During the pluvial, there were five significant El Niño events: 1905, 1906, 1912, 1914, and 1915.

The main evaporative season in all three regions is summer (JJA), and all regions show fairly consistent cool anomalies throughout the pluvial during this season (Figure 5, left panels). In the SW, only 1910 is marginally positive, and the remaining years are all negative, with anomalies on the order of -0.5 to -1 K. Absolute anomalies are even cooler in the NW, matching or exceeding -1 K in five of the pluvial years. In the CP, the cool anomalies start before 1905, averaging about -2 K, and continuing until 1908 with anomalies of about -1 K, coinciding with the earlier start of the pluvial in this region. Afterwards, temperature anomalies are a bit more equivocal, with some major cool years (1912, 1915), but otherwise near-normal temperatures. Over the SW and NW, the major precipitation season is DJF; over CP most precipitation occurs during JJA (Figure 5, right panels). In the SW, there were major positive precipitation anomalies during both the early and later stages of the pluvial; this contrasts with the NW, which showed some minor increases in the beginning, but overall negative precipitation anomalies throughout. Remarkably, only two of the major precipitation years (1914 and 1915) in the SW actually correspond to El Niño events, despite the significant correlation between NINO3.4 and precipitation over this region and season (Pearson's r=+0.33). The other El Niño years (1905, 1906, 1912) are wet in the spring (MAM), although these anomalies are muted relative to DJF (not shown). As with the cool temperature anomalies, the positive precipitation anomalies in the CP begin before 1905. These precipitation anomalies persist through the first four years of the pluvial; after 1908 the CP experiences precipitation deficits every years except for 1915.

c. PDSI: Temperature versus Precipitation

To what extent were the moisture surpluses during the pluvial, as reflected in PDSI, a consequence of enhanced precipitation versus reduced evaporative demand from cool temperature anomalies? To answer this question, we calculate our own PDSI using temperature and precipitation data from the CRU climate grids, spatially averaging over the three regions (Figure 6, top row). We expect these PDSI values to differ somewhat from the NADA PDSI in Figure 2, as we use a different standardization period than the NADA and also a different underlying data set in our calculation (i.e., we calculate PDSI directly, rather than reconstructing from proxy time series). We also do not use any smoothing filter as in Figure 2, in order to emphasize the year to year variability. Despite these differences, our calculated PDSI is generally quite similar to the NADA, showing the two-phase nature of the pluvial (pre and post 1910) in all three regions and the early start to the pluvial over the CP.

To test the importance of temperature versus precipitation during the pluvial, we alternately substitute climatological values (1961-1990) instead of observed temperature and precipitation into the PDSI calculation. We substitute climatology for all months, rather than specific seasons, to account for minor but potentially important contributions from anomalies outside the main precipitation and evaporation seasons. Substituting climatological temperature (keeping observed precipitation) into the PDSI calculation results in varying impacts across the three regions (Figure 6, center row). The SW changes the least, with most major pluvial years showing nearly the same PDSI anomalies, with some diminished positive anomalies in the post-1910 phase. Over the NW there are major reductions in PDSI across most pluvial years; in the CP the early phase of the pluvial truncates earlier. Calculations with climatological precipitation and observed temperatures (Figure 6, bottom row) have a large effect on PDSI values in the SW, essentially converting the pluvial to near normal conditions. In the NW there is a reduction in positive PDSI, although not to the same level as in the climatological temperature scenario. In the CP, substitution of climatological precipitation actually seems to enhance the pluvial, muting early PDSI anomalies slightly but completely eliminating the later drought years during the second half of the pluvial. From these results we conclude that the causes of the moisture surpluses varied across these three regions, driven by high precipitation (SW), low evaporative demand (CP), or a combination of both (NW).

Cool temperature anomalies, and the accompanying low evaporative demand, appear to be an important factor in the pluvial moisture surpluses. However, this explanation depends on the cool temperatures not being either 1) an artifact arising from their occurrence near the beginning of the twentieth century warming trends or 2) a result of increased precipitation, which would make things wet and cool by favoring latent over sensible heating at the surface. A look at global and hemispheric temperatures for the late nineteenth to early twentieth century shows that temperature anomalies during the pluvial period were cool even relative to previous decades (Figure 7) and thus not likely a statistical artifact related to historical warming trends. For all three regions there is a significant ($p<0.05$) negative relationship between precipitation and temperature (Figure 8). However, when the pluvial years are isolated (blue dots), we see that temperatures are near normal or cool (left side of the dashed line), regardless of the precipitation anomalies. This gives strong evidence to reject the second explanation and conclude that the temperature anomalies during the pluvial were largely independent from the precipitation anomalies, allowing them to be an independent causal factor for the pluvial moisture surpluses.

d. Sea Surface Temperatures

Drought and pluvial events over western NA are largely modulated by variations in SSTs, originating primarily from the tropical Pacific (Seager et al. 2005b), part of a zonally and hemispherically symmetric pattern of global hydroclimatic variability (Seager et al. 2003, 2005a). Increased precipitation in the SW is associated with warm-phase El Niño events while cold-phase La Niña events typically suppress precipitation over the same region. The sign of ENSO-precipitation teleconnections is reversed in the NW, with El Niño events leading to drier than normal conditions. The influence of the tropical Pacific is typically strongest during boreal winter.

Composited DJF SST anomalies from all El Niño events (defined as NINO3.4 index $\geq +0.5$ standard deviation) over the last 130 years are shown in the top panel of Figure 9. During El Niño events, warm SST anomalies extend across most of the tropical Pacific, flanked by cool SSTs in the extratropical central north and south Pacific ocean basins. Warm SSTs also typically occur in a narrow band along the west coast of NA. Averaged across all years during the pluvial, SSTs were globally cooler than normal (Figure 9, bottom panel) and the tropical Pacific is near normal, despite the occurrence of five El Niño events (1905, 1906, 1912, 1914, 1915). Even during the pluvial El Niño events, off-equatorial SST anomalies in the Pacific deviate from the expected El Niño pattern, especially in the extratropical north Pacific which was nearly universally cool across the entire basin (not shown). Coupled with the major precipitation surpluses in the SW during off El Niño years, this suggests that El Niño forcing may be insufficient to satisfyingly explain the full pluvial anomalies. The tropical North Atlantic was also cooler than normal during the pluvial, a condition that is typically associated with increased precipitation in central NA (Enfield et al. 2001; Kushnir et al. 2010; Mo et al. 2009).

e. Atmospheric Circulation Anomalies

The influence of tropical Pacific SSTs on NA hydroclimate is communicated via atmospheric circulation responses that act to either enhance or suppress precipitation. In the typical response to El Niño, positive geopotential height anomalies in the tropical/subtropical Pacific and over northern NA flank negative height anomalies near the Gulf of Alaska (Figure 10, top panel). The negative heights drive anomalous cyclonic circulation favoring southerly flows of heat and moisture into western NA which, when coupled with increased ascending motions, act to enhance precipitation. When averaged over the duration of the pluvial (Figure 10, bottom panel), the negative height anomalies are weaker and shifted eastward, while the positive heights over NA shift southeast, extending over eastern NA and Mexico. Compared to the all El Niño composite, this shifts the southerly flow to a more southwesterly track, a configuration highly favorable for so-called “Pineapple Express” winter time storm events (Dettinger 2004). An examination of heights over the subtropical North Atlantic (not shown) shows the absence of a low-level high-pressure anomaly that would be expected if cold North Atlantic SSTs were driving precipitation increases in NA.

Temperature anomalies over NA during the various seasons may be explained, at least partially, by the circulation anomalies (Figure 11). During DJF, positive heights over eastern NA would favor anticyclonic circulation, bringing relatively warm air from the Atlantic onto the continent and warming southeastern NA. The high pressure anomaly over the southwest during JJA would have had a similar advective impact, in this case moving relatively cool air from the Pacific into northwestern NA. Neither feature is typical of a standard El Niño circulation response.

f. GCM Experiments

Circulation anomalies during the pluvial show various features that are alternately consistent and distinct from the expected atmospheric response to El Niño forcing. Since El Niño may be insufficient to fully explain the pluvial climate and atmospheric response, it is useful to determine to what extent these other anomalies are forced by SSTs or arise from other processes in the climate system. To investigate this, we leverage the GCM simulations described previously to look at the climate response over NA to global observed SSTs during the pluvial. Model results shown are the mean of a 16-member ensemble, representing the SST-forced component of model variability.

Geopotential heights composited from all El Niño years in the GCM ensemble show that the model does a good job reproducing the major circulation features associated with El Niño in the reanalysis (Figure 12, top panel), although with somewhat weaker amplitudes

(Figure 10, top panel). During the pluvial, however, the pattern of the model heights diverges from the reanalysis, and seems to simply reflect the imprint of the five El Niño events (Figure 12, bottom panel). In the model composite, the positive height anomalies over the western North Pacific and eastern NA are absent, and the major region of negative heights is centered over the ocean, rather than being shifted to the east over the west coast of NA as it is in the reanalysis. The precipitation anomalies from the model largely reflect the influence of El Niño events in the mean pluvial circulation, with enhanced precipitation in the SW and Mexico in DJF and MAM (Figure 13). These anomalies, however, are muted compared to observations (Figure 4), and have slightly different spatial patterns. For example, model precipitation anomalies during DJF are shifted too far to the south, and the major precipitation increases occur in MAM, rather than DJF. Temperature anomalies from the GCM ensemble (Figure 14) are cool but muted compared to the observations. The model also does not reproduce the observed spatial structure in the temperature anomalies.

In a recent study, Cook et al. (in press) used a statistical drought model to investigate SST forcing of persistent multi-year twentieth century hydroclimatic events over western NA, including the pluvial. Using statistical modes representing drought variability associated with tropical and extratropical Pacific SSTs, they were able to reproduce the magnitude and spatial pattern of the pluvial above random noise in over 95% of their model ensemble members, with an anomaly correlation between the ensemble median modeled drought pattern and observations of 0.76. Their conclusion, that knowledge of tropical and extratropical Pacific SSTs should be sufficient to predict the pluvial, appears to be at odds with results from our GCM simulations which seem unable to fully resolve the important circulation and precipitation anomalies.

The role of extratropical north Pacific SSTs in forcing hydroclimatic variability over NA is controversial because SST variability in the extratropical north Pacific is primarily forced by the atmosphere (Deser et al. 2010). In the statistical model, the SST mode of drought variability associated with the extratropical North Pacific may simply reflect fortuitous atmospheric circulation patterns associated with internal atmospheric variability, or could be a high-latitude expression of ocean variability linked to dynamics in the tropical Pacific (An et al. 2007; Schneider and Cornuelle 2005). This would result in overfitting of the statistical model and an overestimation of the SST-forced component of the pluvial. On longer timescales than ENSO, Pacific SST variability is dominated by the Pacific Decadal Oscillation (PDO), or Pacific Decadal Variability (PDV), which has a strong expression in the North Pacific Ocean (Mantua et al. 1997; Zhang et al. 1997). Much work has been done, mostly of an observational nature, suggesting that NA hydroclimate can be influenced by the PDO (e.g., Gershunov and Barnett 1998; Goodrich 2007; McCabe et al. 2004, 2008). For example, differences in a variety of hydroclimatic variables can be seen in western NA between positive and negative phases of the PDO, even when only neutral ENSO years are considered (e.g., Goodrich 2007). And for various combinations of PDO and ENSO phases, drought and pluvial anomalies can be either amplified or diminished (e.g., Kurtzman and Scanlon 2007). However, the PDO is also associated with strong tropical Pacific SST anomalies (Zhang et al. 1997) and these PDO-hydroclimate links could be explained by the tropical SST anomalies. Indeed, no modeling study to date has demonstrated that any appreciable portion of the hydroclimate history of North America is explained as a response to extratropical SST anomalies either in the Pacific or Atlantic Oceans. Hence it is curious that Fye et al. (2004) surmised the atmospheric circulation anomalies during the pluvial using only North Pacific SST information, conjecturing that the combined warm tropical Pacific and cold north Pacific would lead to anticyclonic anomalies over the western north Pacific and a long-wave trough centered near the west coast of NA. While the physical basis for why this would happen is unclear, these circulation features are clearly shown in Figure 10. It could be that this GCM, like others, potentially misses an impact of SST anomalies in the extratropical Pacific on hydroclimatic variability over NA (which are implicitly resolved within a statistical framework) or it could be that the circulation anomalies important to the pluvial were a combination of El Niño forcing with a large dose of internal atmospheric variability. Only more work, including simulation with other GCMs, may be able to resolve this issue.

4. Discussion and Conclusions

Throughout history, persistent periods of extreme climate have significantly impacted the functioning of societies, and have often been instrumental in shaping resource use policies and societal reorganizations (e.g., Buckley et al. 2010; Hansen and Libecap 2004). One such event, the early twentieth century pluvial, set up unrealistic expectations for water availability in western NA, leading to development trajectories that surpassed the long-term support capacity defined by the climatology of the region (Christensen et al. 2004). Increasing our understanding of the causes and dynamics of this, and other, climate events can help us place current and future climate changes in the proper context and inform how we deal with these events at the societal level. The specific goal of this study was to investigate the causes of the moisture surpluses during the early twentieth century pluvial, and determine how well anomalies during that time fit into our understanding of NA hydroclimatic variability. Our main results are summarized:

- Across the west, the origin of the moisture surpluses during the pluvial varied by region and can be attributed primarily to increased precipitation (the SW), decreased evaporative demand (the CP), or a combination of the two (the NW).
- El Niño played a partial role in the pluvial moisture surpluses, contributing primarily to increased moisture convergence and precipitation in the SW. However, other anomalies in the SST, circulation, and precipitation anomaly fields diverged from the expected El Niño response.
- The intensity and spatial extent of the pluvial can be well reproduced using a statistical model with conceptualized tropical and extratropical Pacific SST forcing (Cook et al. in press). An independent GCM simulation driven by SST observations produces the El Niño response observed during the pluvial, but is incapable of simulating other important features.

Studies of pluvial events (e.g., Schubert et al. 2008; Seager et al. 2005b) in the climate literature are relatively rare when compared to the wealth of drought investigations, an understandable asymmetry given the typically larger impacts and costs of droughts. Extensive research into drought variability over North America has helped illuminate the role of SST variability in the ENSO region, and highlighted the importance of La Niña events as major drivers of persistent drought in the west (e.g., Seager et al. 2005b). For the early twentieth century pluvial, however, our investigation indicates that SSTs in the ENSO region had relatively little explanatory power. This suggests that it may be wrong to conceptualize persistent pluvials as simply the opposite of droughts, and that they may possess characteristics unrelated to ENSO variability (e.g., cool temperatures) that are important for driving moisture surpluses. Research into pluvial dynamics is limited, however, by the paucity of extended pluvial events that have occurred during the instrumental period.

The discrepancy between the statistical model and the GCM also highlights some of the uncertainties and the often disparate conclusions reached by empirical (McCabe et al. 2004, 2008) versus model based (Seager et al. 2005b; Seager 2007) investigations of North American hydroclimatic variability. Specifically, the two camps disagree on the efficacy of extratropical North Pacific forcing of NA hydroclimate with the GCM experiments indicating the dominance of tropical forcing. Reducing this key uncertainty will require further studies exploiting both empirical analyses and modeling.

Acknowledgments.

The authors thank X anonymous reviews for comments that significantly improved the quality of this manuscript. Twentieth Century Reanalysis V2 data provided by the NOAA/OAR/ESRL PSD, Boulder, Colorado, USA, from their Web site at `http://www.esrl.noaa.gov/psd/`. Support for the Twentieth Century Reanalysis Project dataset is provided by the U.S. Department of Energy, Office of Science Innovative and Novel Computational Impact on Theory and Experiment (DOE INCITE) program, and Office of Biological and Environmental Research (BER), and by the National Oceanic and Atmospheric Administration Climate Program Office. Lamont Contribution XXXX.

REFERENCES

An, S., J. Kug, A. Timmermann, I. Kang, and O. Timm, 2007: The Influence of ENSO on the Generation of Decadal Variability in the North Pacific*. *Journal of Climate*, **20 (4)**, 667–680.

Barnett, T. and D. Pierce, 2009: Sustainable water deliveries from the Colorado River in a changing climate. *Proceedings of the National Academy of Sciences*, **106 (18)**, 7334.

Brohan, P., J. Kennedy, I. Harris, S. Tett, and P. Jones, 2006: Uncertainty estimates in regional and global observed temperature changes: A new data set from 1850. *Journal of Geophysical Research-Atmospheres*, **111 (D12)**, D12 106.

Buckley, B., et al., 2010: Climate as a contributing factor in the demise of Angkor, Cambodia. *Proceedings of the National Academy of Sciences*, **107 (15)**, 6748.

Christensen, N., A. Wood, N. Voisin, D. Lettenmaier, and R. Palmer, 2004: The effects of climate change on the hydrology and water resources of the Colorado River basin. *Climatic Change*, **62 (1)**, 337–363.

Compo, G., J. Whitaker, and P. Sardeshmukh, 2006: Feasibility of a 100-year reanalysis using only surface pressure data. *Bulletin of the American Meteorological Society*, **87 (2)**, 175–190.

Compo, G., et al., submitted: The Twentieth Century Reanalysis Project. *Quarterly Journal of the Royal Meteorological Society*.

Cook, B., E. Cook, K. Anchukaitis, R. Seager, and R. Miller, in press: Forced and unforced variability of twentieth century North American droughts and pluvials. *Climate Dynamics*, DOI 10.1007/s00 382–010–0897–9.

Cook, B., R. Seager, and R. Miller, 2010: Atmospheric circulation anomalies during two persistent north american droughts: 1932-1939 and 1948-1957. *Climate Dynamics*, **in press (DOI: 10.1007/s00382-010-0807-1)**.

Cook, E., D. Meko, D. Stahle, and M. Cleaveland, 1999: Drought Reconstructions for the Continental United States*. *Journal of Climate*, **12 (4)**, 1145–1162.

Cook, E., R. Seager, M. Cane, and D. Stahle, 2007: North American drought: Reconstructions, causes, and consequences. *Earth Science Reviews*, **81 (1-2)**, 93–134.

Cook, E., C. Woodhouse, C. Eakin, D. Meko, and D. Stahle, 2004: Long-Term Aridity Changes in the Western United States. *Science*, **306 (5698)**, 1015–1018.

Deser, C., M. Alexander, S. Xie, and A. Phillips, 2010: Sea Surface Temperature Variability: Patterns and Mechanisms. *Annu. Rev. Mar. Sci*, **2**, 115–43.

Dettinger, M., 2004: Fifty-two years of "pineapple-express" storms across the West Coast of North America. Tech. rep., US Geological Survey, Scripps Institution of Oceanography for the California Energy Commission.

Dracup, J., K. Lee, and E. Paulson Jr, 1980: On the definition of droughts. *Water Resources Research*, **16 (2)**, 297–302.

Enfield, D., A. Mestas-Nunez, and P. Trimble, 2001: The Atlantic Multidecadal Oscillation and its relationship to rainfall and river flows in the Continental US. *Geophys. Res. Lett*, **28**, 2077–2080.

Fye, F., D. Stahle, and E. Cook, 2003: Paleoclimatic analogs to twentieth-century moisture regimes across the United States. *Bulletin of the American Meteorological Society*, **84 (7)**, 901–909.

Fye, F., D. Stahle, and E. Cook, 2004: Twentieth-Century Sea Surface Temperature Patterns in the Pacific during Decadal Moisture Regimes over the United States. *Earth Interactions*, **8**, 1–22.

Gershunov, A. and T. Barnett, 1998: Interdecadal modulation of ENSO teleconnections. *Bulletin of the American Meteorological Society*, **79 (12)**, 2715–2725.

Goodrich, G., 2007: Influence of the Pacific decadal oscillation on winter precipitation and drought during years of neutral ENSO in the western United States. *Weather and forecasting*, **22 (1)**, 116–124.

Hansen, Z. and G. Libecap, 2004: Small Farms, Externalities, and the Dust Bowl of the 1930s. *Journal of Political Economy*, **112 (3)**, 665–694.

Herweijer, C., R. Seager, E. Cook, and J. Emile-Geay, 2007: North American Droughts of the Last Millennium from a Gridded Network of Tree-Ring Data. *Journal of Climate*, **20 (7)**, 1353–1376.

Kaplan, A., M. Cane, Y. Kushnir, A. Clement, M. Blumenthal, and B. Rajagopalan, 1998: Analyses of global sea surface temperature 1856-1991. *Journal of Geophysical Research*, **103 (18)**, 567–18.

Kiehl, J., J. Hack, G. Bonan, B. Boville, D. Williamson, and P. Rasch, 1998: The National Center for Atmospheric Research Community Climate Model: CCM3*. *Journal of Climate*, **11 (6)**, 1131–1149.

Kurtzman, D. and B. Scanlon, 2007: El Niño–Southern Oscillation and Pacific Decadal Oscillation impacts on precipitation in the southern and central United States: Evaluation of spatial distribution and predictions. *Water Resources Research*, **43 (10)**, W10 427.

Kushnir, Y., R. Seager, M. Ting, N. Naik, and J. Nakamura, 2010: Mechanisms of Tropical Atlantic SST Influence on North American Hydroclimate Variability. *Journal of Climate*, doi: 10.1175/2010JCLI3172.1.

MacDonnell, L., D. Getches, and W. Hugenberg Jr, 1995: The law of the Colorado River: Coping with severe sustained drought. *Water Resources Bulletin*, **31 (5)**, 825–836.

Mantua, N., S. Hare, Y. Zhang, J. Wallace, and R. Francis, 1997: A Pacific Interdecadal Climate Oscillation with Impacts on Salmon Production. *Bulletin of the American Meteorological Society*, **78 (6)**, 1069–1079.

McCabe, G., J. Betancourt, S. Gray, M. Palecki, and H. Hidalgo, 2008: Associations of multidecadal sea-surface temperature variability with US drought. *Quaternary International*, **188 (1)**, 31–40.

McCabe, G., M. Palecki, and J. Betancourt, 2004: Pacific and Atlantic Ocean influences on multidecadal drought frequency in the United States. *Proceedings of the National Academy of Sciences*, **101 (12)**, 4136–4141.

Meko, D., C. Woodhouse, C. Baisan, T. Knight, J. Lukas, M. Hughes, and M. Salzer, 2007: Medieval drought in the upper Colorado River Basin. *Geophysical Research Letters*, **34 (10)**, 10 705–10 709.

Mitchell, T. and P. Jones, 2005: An improved method of constructing a database of monthly climate observations and associated high-resolution grids. *Int. J. Climatol*, **25 (6)**, 693–712.

Mo, K., J. Schemm, and S. Yoo, 2009: Influence of ENSO and the Atlantic Multidecadal Oscillation on Drought over the United States. *Journal of Climate*, **22**, 5962–5982.

Palmer, W., 1965: Meteorological drought. *Research paper*, **45**, 1–58.

Rayner, N., D. Parker, E. Horton, C. Folland, L. Alexander, D. Rowell, E. Kent, and A. Kaplan, 2003: Global analyses of sea surface temperature, sea ice, and night marine air temperature since the late nineteenth century. *J. Geophys. Res*, **108 (D14)**, 4407.

Reisner, M., 1993: *Cadillac desert: the American West and its disappearing water*. Penguin Group USA.

Schneider, N. and B. Cornuelle, 2005: The Forcing of the Pacific Decadal Oscillation. *Journal of Climate*, **18 (21)**, 4355–4373.

Schubert, S., M. Suarez, P. Pegion, R. Koster, and J. Bacmeister, 2008: Potential predictability of long-term drought and pluvial conditions in the US Great Plains. *Journal of Climate*, **21 (4)**, 802–816.

Seager, R., 2007: The Turn of the Century North American Drought: Global Context, Dynamics, and Past Analogs. *Journal of Climate*, **20 (22)**, 5527–5552.

Seager, R., N. Harnik, Y. Kushnir, W. Robinson, and J. Miller, 2003: Mechanisms of hemispherically symmetric climate variability. *Journal of Climate*, **16 (18)**, 2960–2978.

Seager, R., N. Harnik, W. Robinson, Y. Kushnir, M. Ting, H. Huang, and J. Velez, 2005a: Mechanisms of ENSO-forcing of hemispherically symmetric precipitation variability. *Quarterly Journal of the Royal Meteorological Society*, **131 (608)**.

Seager, R., Y. Kushnir, C. Herweijer, N. Naik, and J. Velez, 2005b: Modeling of Tropical Forcing of Persistent Droughts and Pluvials over Western North America: 1856–2000. *Journal of Climate*, **18 (19)**, 4065–4088.

Sophocleous, M., 2010: Review: groundwater management practices, challenges, and innovations in the High Plains aquifer, USA—lessons and recommended actions. *Hydrogeology Journal*, **18 (3)**, 559–575.

Stockton, C. and G. Jacoby, 1976: Long-Term Surface-Water Supply and Streamflow Trends in the Upper Colorado River Basin. *Lake Powell Research Project Bulletin*, **1 (18)**.

Whitaker, J., G. Compo, X. Wei, and T. Hamill, 2004: Reanalysis without radiosondes using ensemble data assimilation. *Monthly Weather Review*, **132**, 1190–1200.

Wood, K. and J. Overland, 2009: Early 20th century arctic warming in retrospect. *International Journal of Climatology*, **Early View**.

Woodhouse, C., K. Kunkel, D. Easterling, and E. Cook, 2005: The twentieth-century pluvial in the western United States. *Geophysical Research Letters*, **32 (7)**, L07 701.

Worster, D., 1992: *Rivers of empire: Water, aridity, and the growth of the American West*. Oxford University Press, USA.

Zhang, Y., J. Wallace, and D. Battisti, 1997: ENSO-like interdecadal variability: 1900-93. *Journal of Climate*, **10 (5)**, 1004–1020.

List of Figures

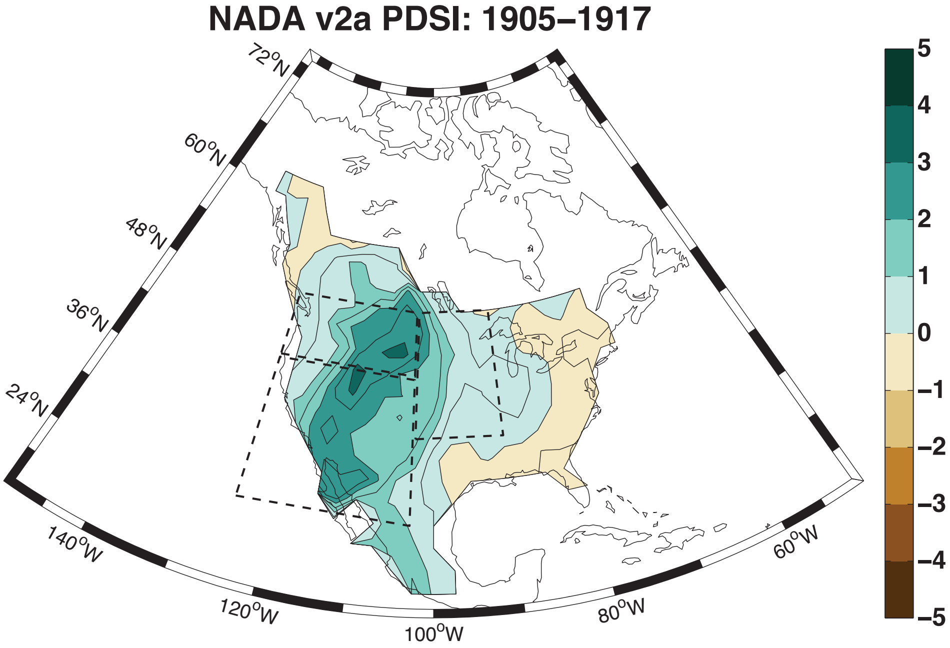

Fig. 1. Summer season (June-July-August, JJA) PDSI anomalies from the NADA, averaged across all pluvial years (1905-1917).

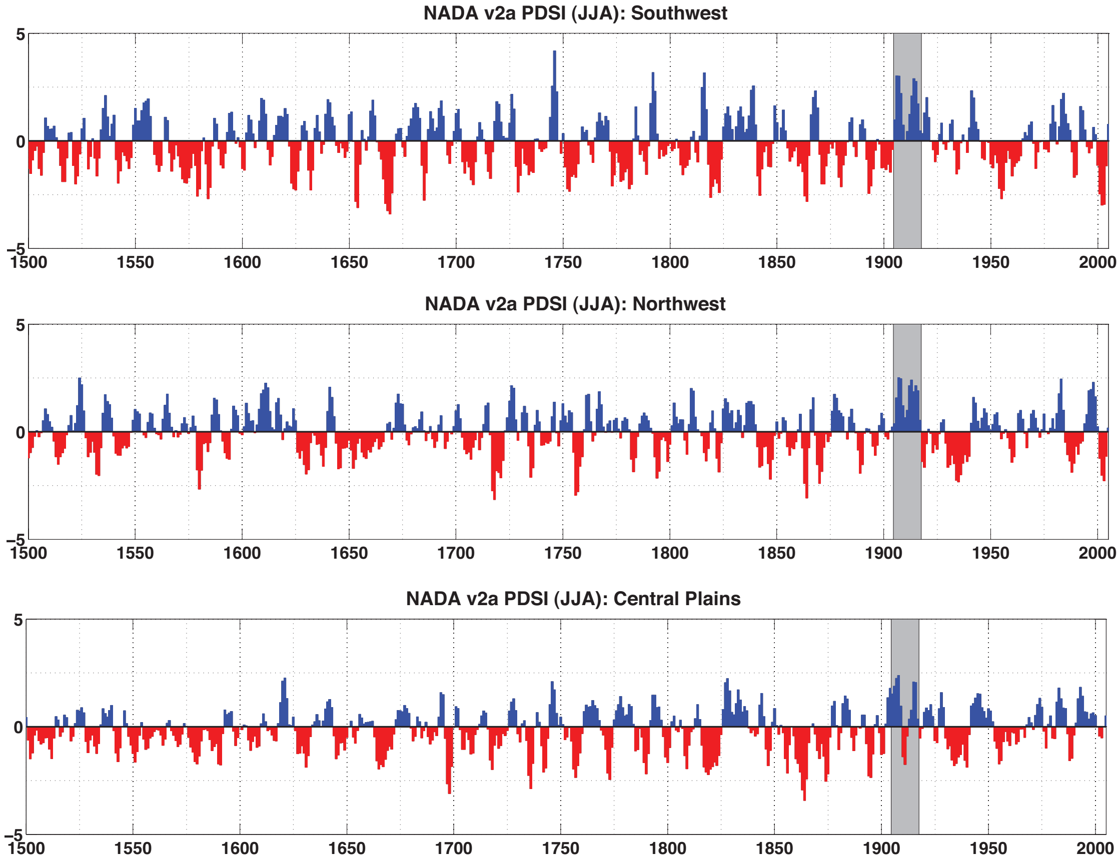

FIG. 2. Area averaged summer season (June-July-August, JJA) PDSI from the NADA v2a for 1500-2005. All time series are smoothed with a five year lowess filter. Time series correspond to the outlined boxes in Figure 1: the southwest (SW; 125°W-103°W, 25°N-42°N), the northwest (NW; 125°W-103°W, 42°N-50°N), and the central plains (CP; 103°W-90°W, 35°N-50°N).

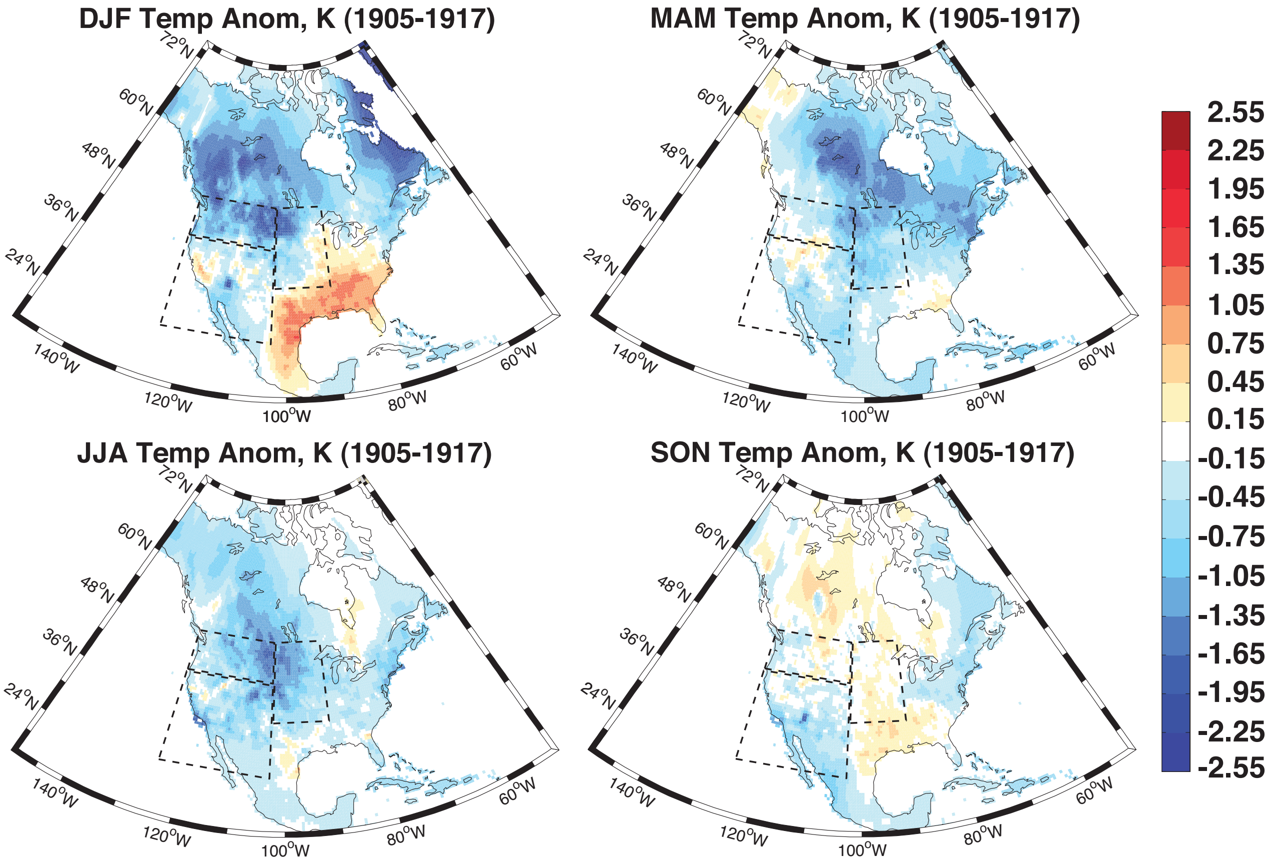

FIG. 3. Seasonal temperature anomalies during 1905-1917 from the CRU 2.1 climate grids, relative to the 1961-1990 mean (K).

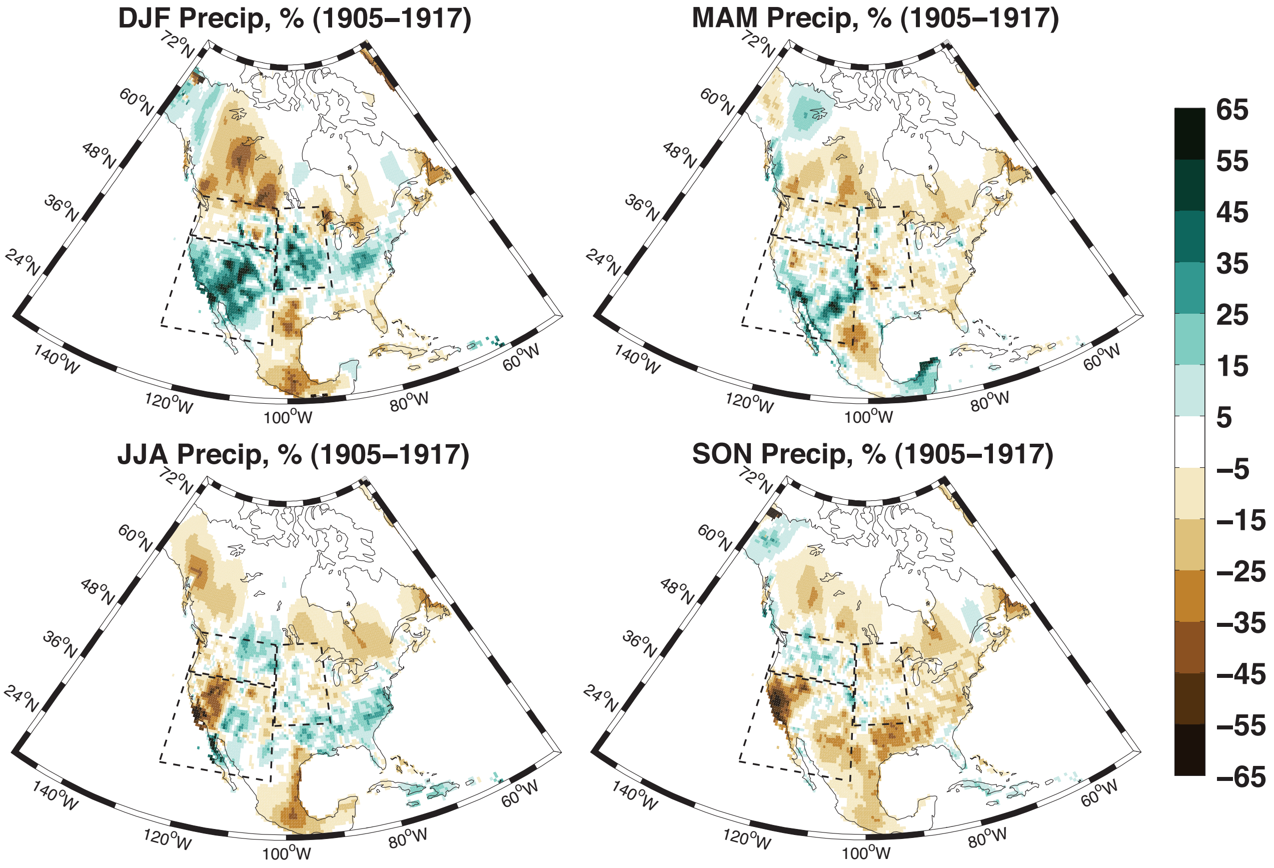

Fig. 4. Precipitation anomalies during 1905-1917 from the CRU 2.1 climate grids, expressed as percent difference relative to the 1961-1990 mean.

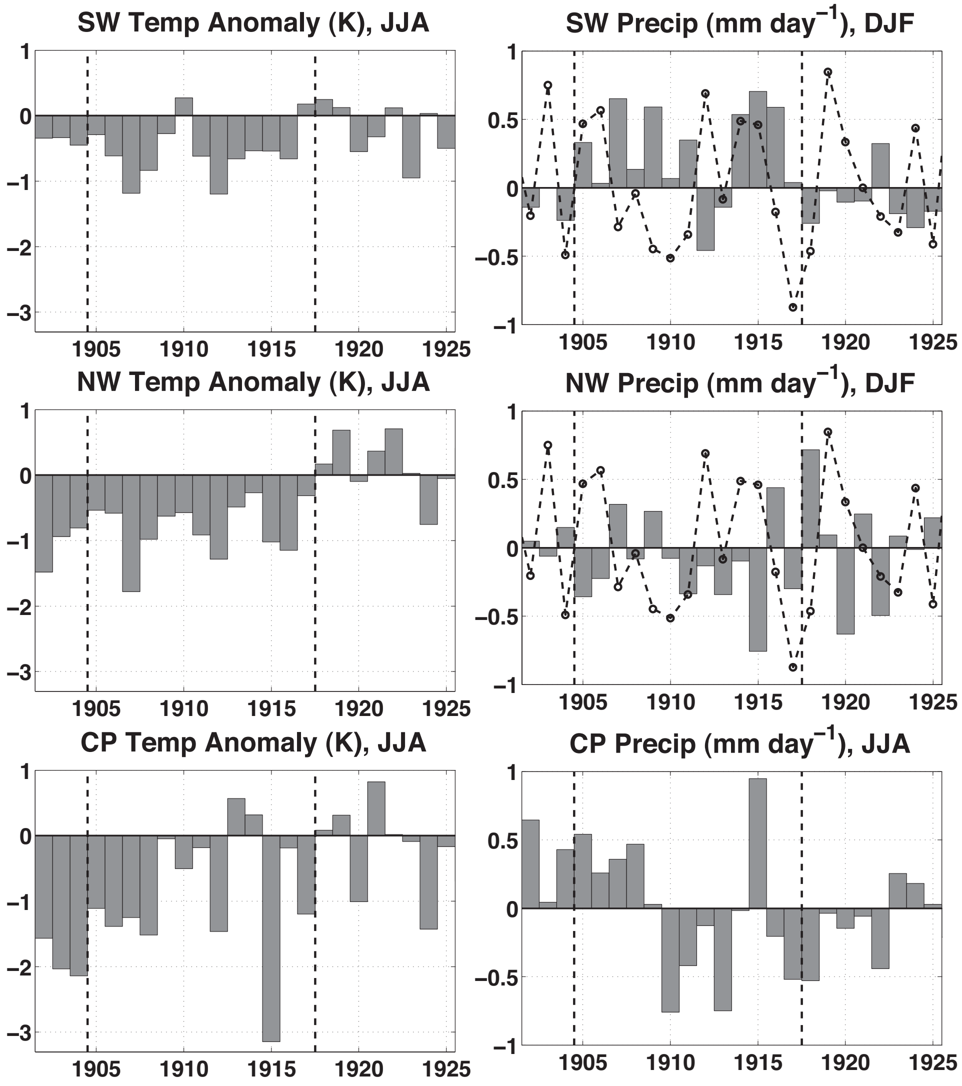

Fig. 5. Temperature (K) and precipitation (mm day^{-1}) anomalies during 1905-1917 for the three outlined regions. The indicated three month seasons represent the main evaporation and precipitation seasons for each region. Dashed lines are a scaled version of the NINO3.4 index, included to indicate the five El Niño years during the pluvial (1905, 1906, 1912, 1914, 1915). All temperature and precipitation anomalies are relative to the 1961-1990 mean.

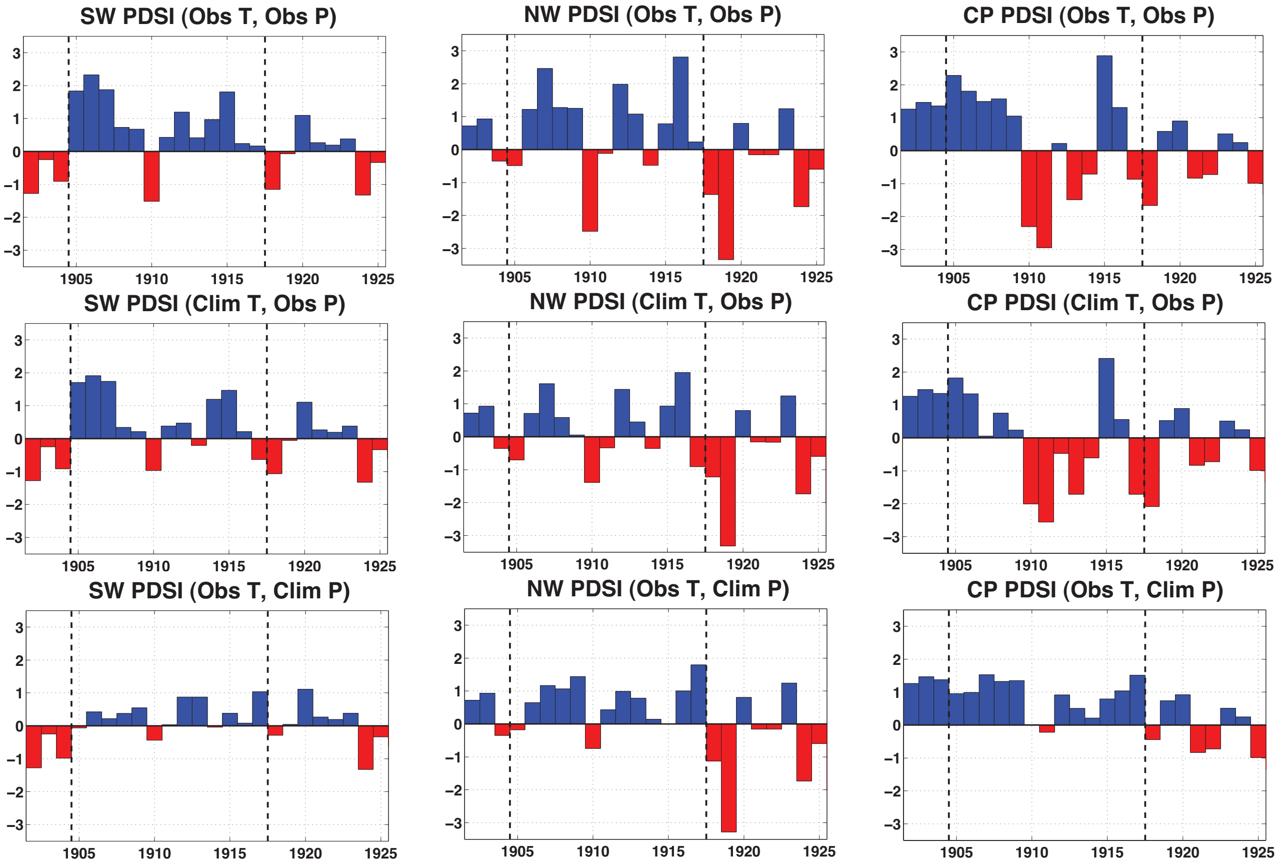

Fig. 6. Summer season (JJA) PDSI calculated from the CRU 2.1 precipitation and temperature climate grids averaged over the southwest (SW, left column), northwest (NW, center column), and central plains (CP, right column). For the pluvial period (1905-1917), PDSI is alternately calculated with observed temperature and observed precipitation (top row), climatological temperature and observed precipitation (center row), and observed temperature and climatological precipitation (bottom row).

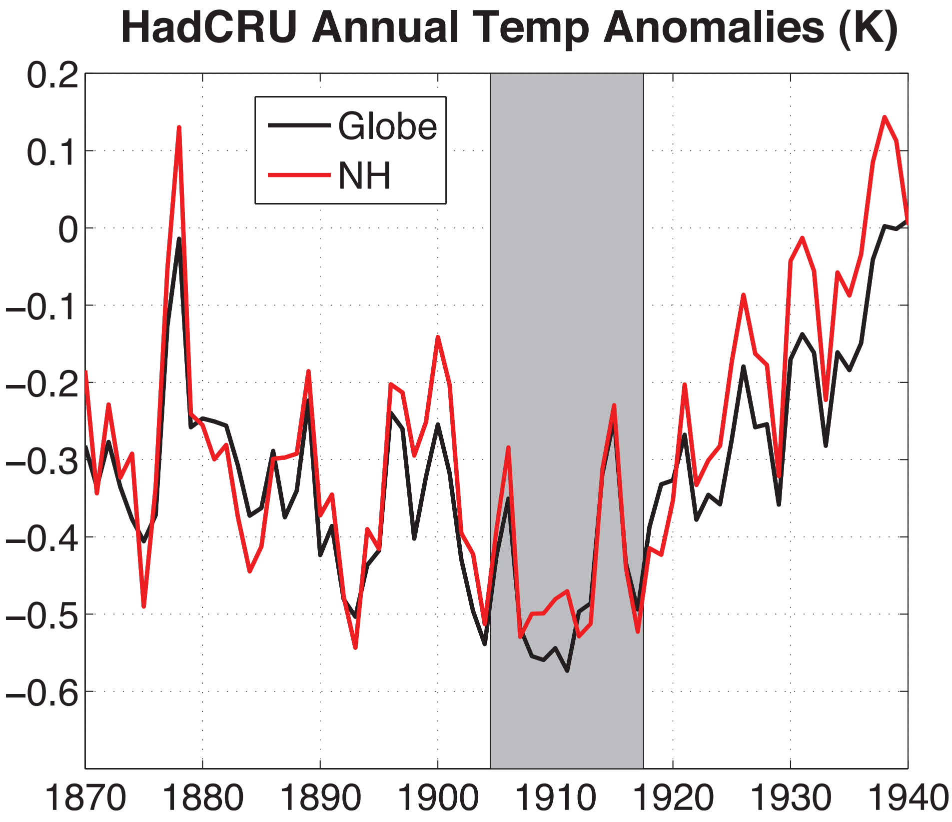

Fig. 7. Global and northern hemisphere averaged surface temperature anomalies (K, from HadCRU), 1870-1940. The 1905-1917 pluvial interval (shaded grey) was relatively cool compared to either the preceding or following decades.

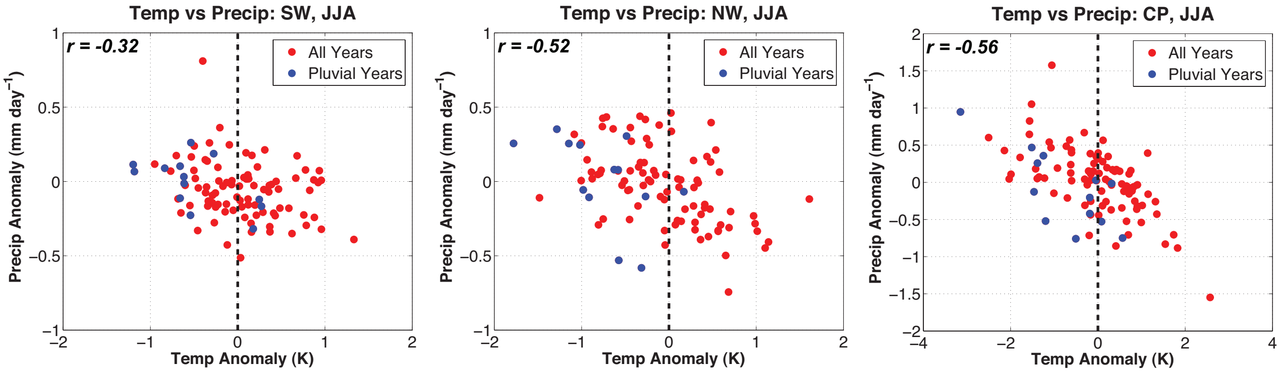

Fig. 8. Summer (JJA) temperature versus precipitation anomalies, averaged over the three regions for 1901-2002 (from the CRU 2.1 climate grids). Years during the pluvial (1905-1917) are colored in blue. Spearman rank correlations between temperature and precipitation are inset each plot.

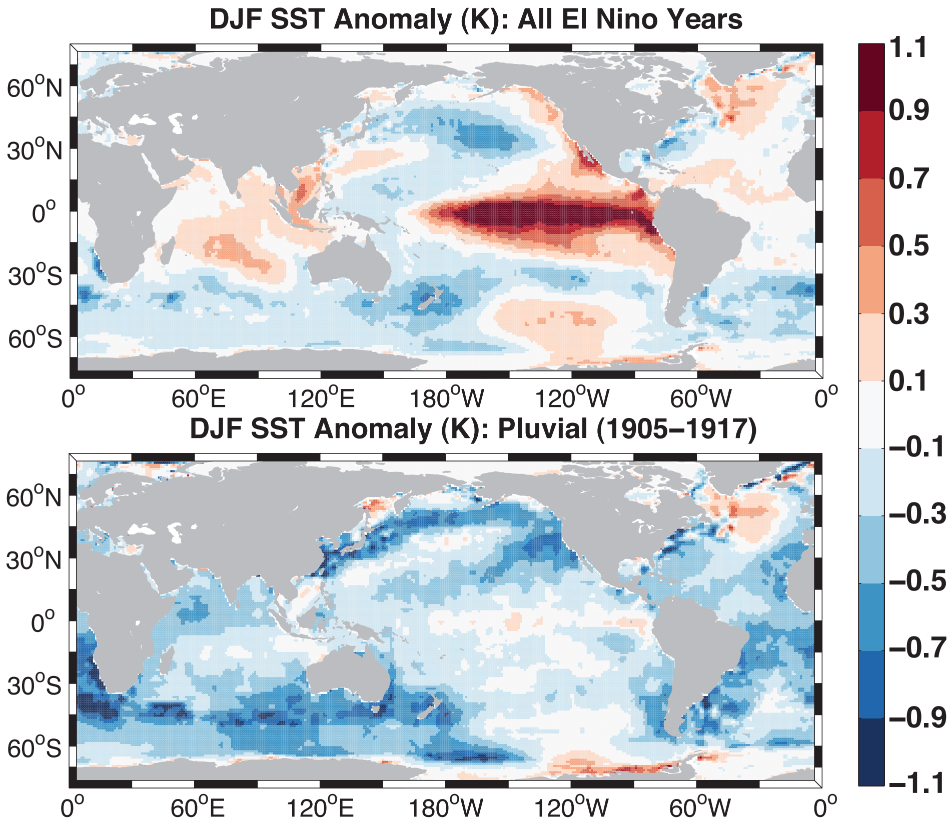

FIG. 9. Composite sea surface temperature anomalies (K, from HadISST v1) for all El Niño years during the instrumental period (top) and all pluvial years (1905-1917; bottom).

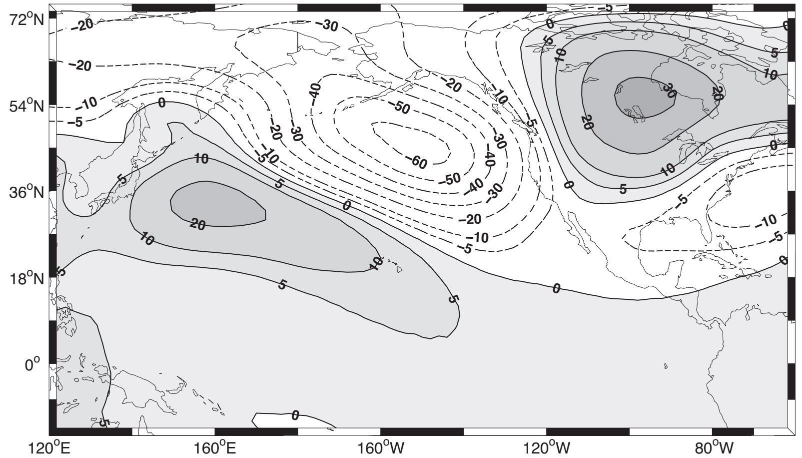

DJF Height Anomaly: 500 hPa, All El Nino Years

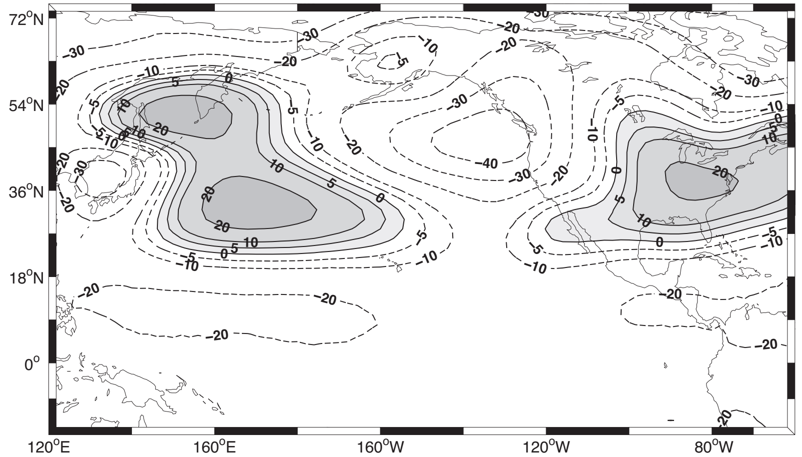

DJF Height Anomaly: 500 hPa, Pluvial (1905–1917)

Fig. 10. Composite 500 hPa geopotential heights (meters) for all El Niño years during the instrumental period (top) and all pluvial years (1905-1917; bottom).

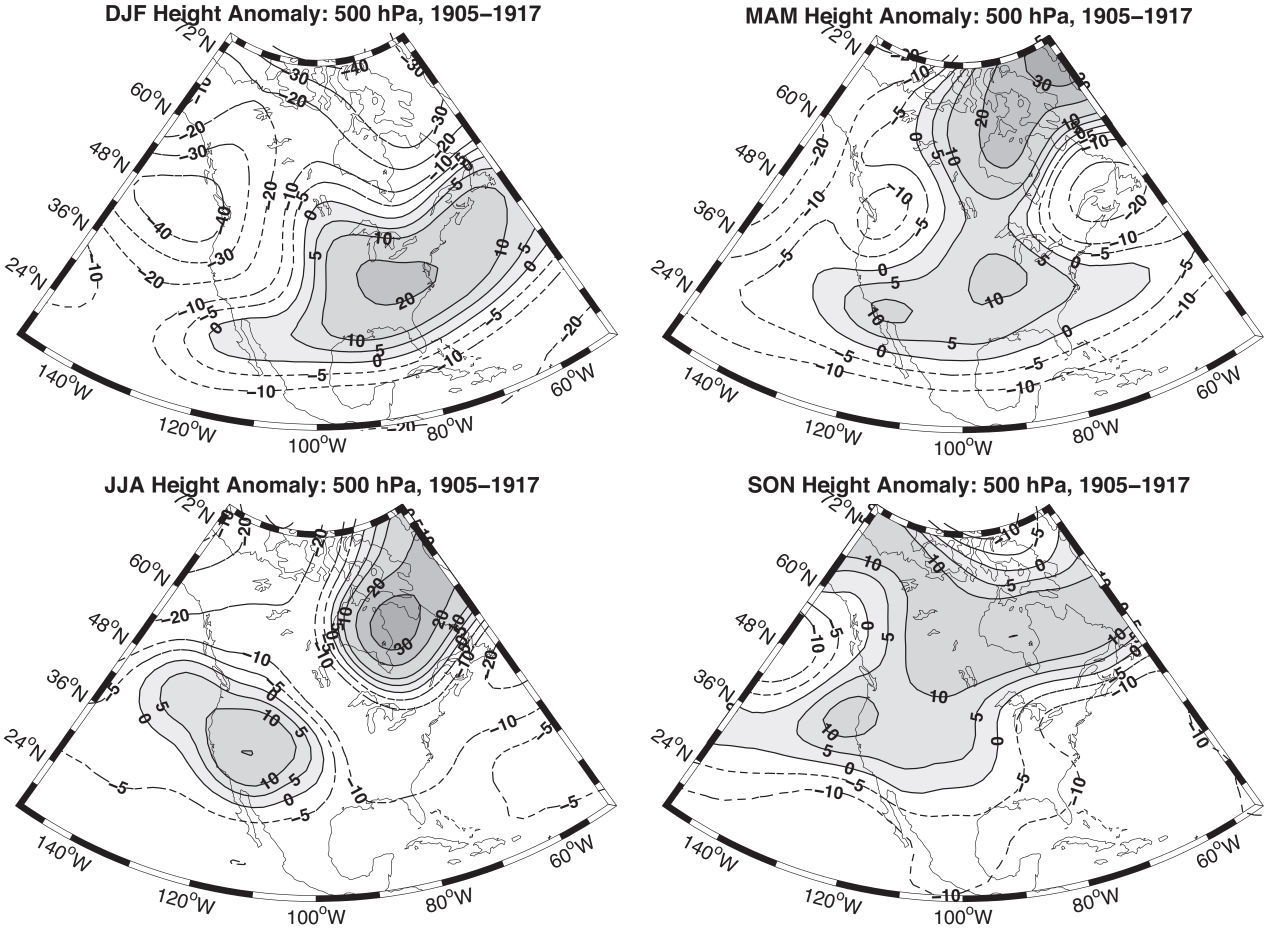

Fig. 11. Composite 500 hPa geopotential heights anomalies (meters), averaged over the pluvial (1905-1917) for each season.

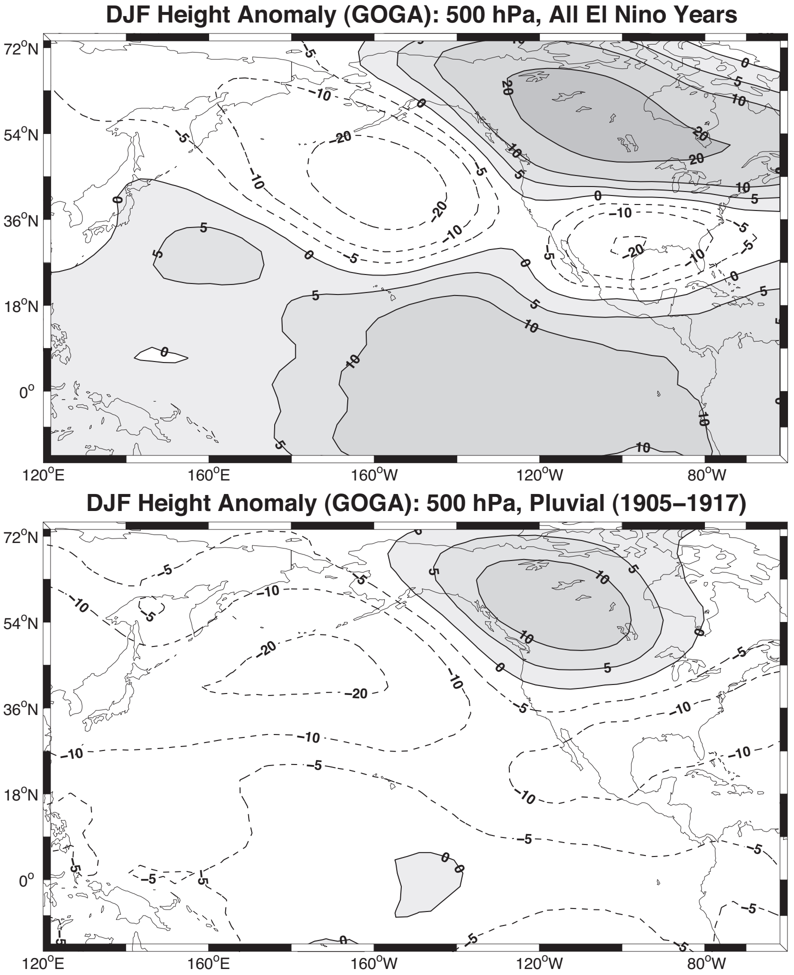

DJF Height Anomaly (GOGA): 500 hPa, All El Nino Years

DJF Height Anomaly (GOGA): 500 hPa, Pluvial (1905–1917)

Fig. 12. Composite 500 hPa geopotential heights (meters) for all El Niño years (top) and all pluvial years (1905-1917; bottom) from the ensemble mean of the GCM simulations.

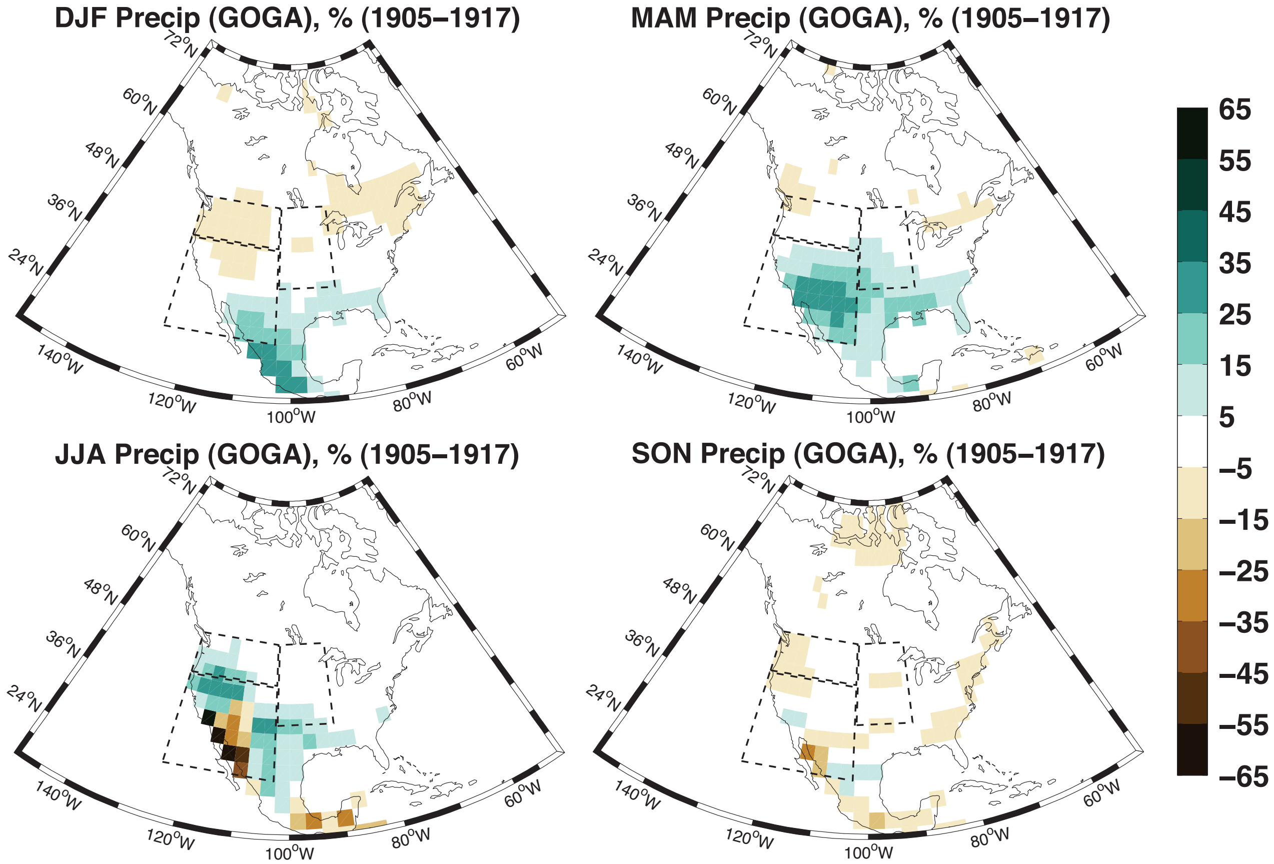

Fig. 13. Precipitation anomalies during 1905-1917 from the ensemble mean of the GCM simulations, expressed as percent difference relative to the 1961-1990 ensemble mean.

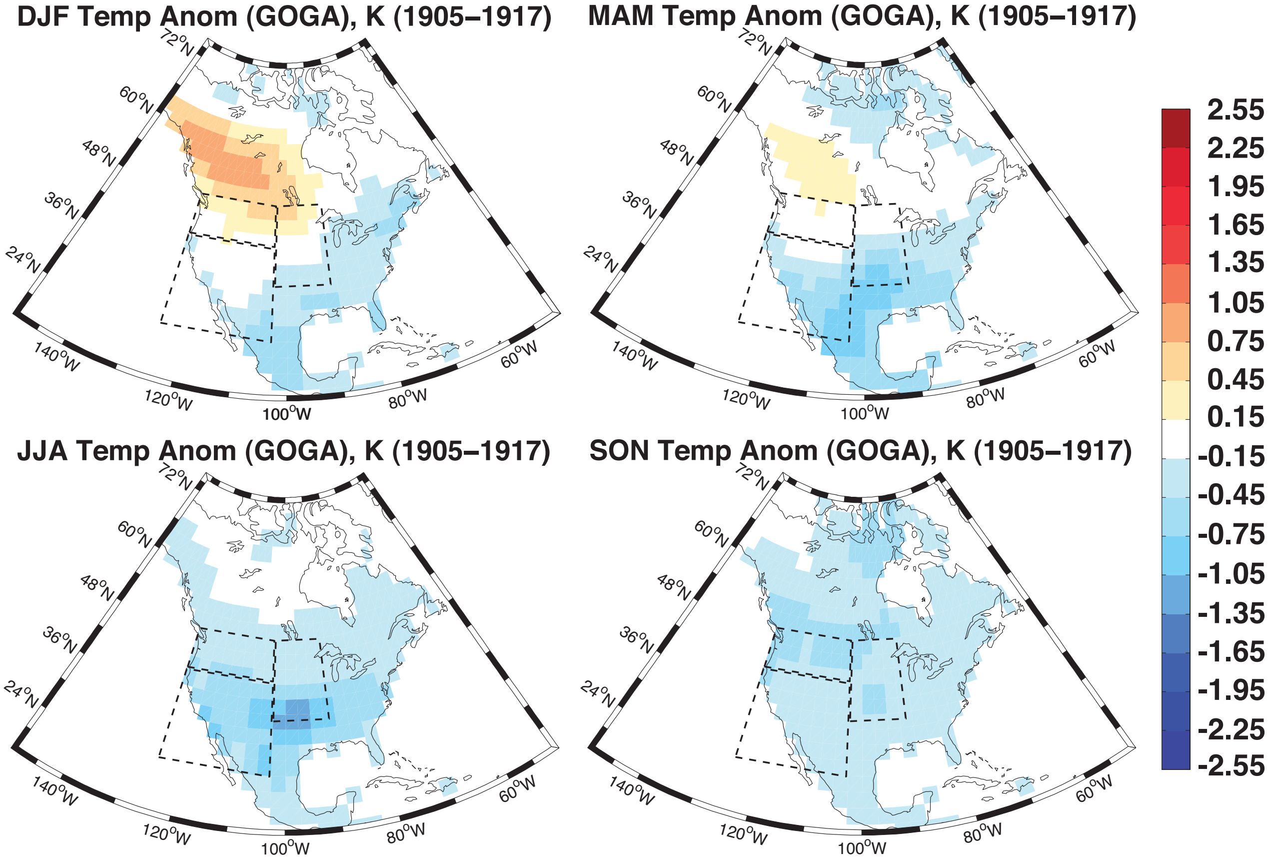

Fig. 14. Temperature anomalies during 1905-1917 from the ensemble mean of the GCM simulations (K), relative to the 1961-1990 ensemble mean.